



# Shape-Designable and Size-Tunable Organic–Inorganic Hybrid Perovskite Micro-Ring Resonator Arrays

Shun-Xin Li, Hong Xia,\* Guo-Ping Zhang, Xiao-Lu Xu, Ying Yang, Gong Wang, and Hong-Bo Sun\*

Micro-ring resonators are widely used in many fields due to their compact structure, high integration, and rich functions. In recent years, perovskite materials have been widely concerned because of their superior properties and various shapes of perovskite-based optical resonators have been achieved. Despite the excellent photoelectric properties of perovskite materials, it is difficult to realize micro-ring resonators based on perovskite materials due to its tendency to crystallize into cubic structures. Here, this problem is solved by a microstructure edge-guided crystallization method to fabricate shape-designable and size-tunable methylammonium lead bromide (MAPbBr<sub>3</sub>) micro-ring resonator arrays with high performance.

In recent years, the development of optoelectronic information technology requires higher integration of optoelectronic devices.<sup>[1–6]</sup> Because of its compact structure, high integration, and rich functions, micro-ring resonators have been considered as one of the best building blocks of photonic integrated systems.<sup>[7–9]</sup> Micro-ring resonators with unique properties such as small volume, multiple functions, and high quality factor have attracted wide attentions in many fields such as optical communication, biochemical sensing, non-linear optics, and quantum optics.<sup>[10–15]</sup> Since it was first proposed in 1969, micro-ring resonators have been successfully achieved in various material systems such as silicon, III-V semiconductor, glass, and polymer by various methods such as electron beam lithography, dry etching, and ultraviolet lithography.<sup>[16–20]</sup> So far, scientists are still exploring new materials to fabricate high quality micro-ring resonators.<sup>[21–23]</sup>

Dr. S.-X. Li, Prof. H. Xia, G.-P. Zhang, X.-L. Xu, Y. Yang, Dr. G. Wang, Prof. H.-B. Sun

State Key Laboratory of Integrated Optoelectronics  
College of Electronic Science and Engineering  
Jilin University  
2699 Qianjin Street, Changchun 130012, China  
E-mail: hxia@jlu.edu.cn

Prof. H.-B. Sun  
State Key Laboratory of Precision Measurement Technology  
and Instruments  
Department of Precision Instrument  
Tsinghua University  
Haidian, Beijing 100084, China  
E-mail: hbsun@tsinghua.edu.cn

 The ORCID identification number(s) for the author(s) of this article can be found under <https://doi.org/10.1002/admt.202000051>.

DOI: 10.1002/admt.202000051

Perovskite materials have attracted widespread attention due to their excellent photoelectric properties and have been considered as an important material for many optoelectronic devices.<sup>[24–29]</sup> For example, Xiong group had successfully achieved room-temperature near-infrared perovskite planar nanolasers in perovskite nanoplatelets.<sup>[30]</sup> Despite the exciting progress of perovskite-based resonators such as micro-disks,<sup>[31–34]</sup> micro-wires,<sup>[35,36]</sup> micro-spheres,<sup>[37,38]</sup> and so on,<sup>[39]</sup> attributed to the fact that perovskite materials tend to crystallize into cubic shaped microcrystals, it is more difficult to form a curved ring

structure.<sup>[40]</sup> Although the preparation methods of micro-rings in other materials are becoming more and more mature,<sup>[41–44]</sup> there are few reports on perovskite micro-ring resonators.<sup>[45]</sup> Due to the instability of perovskite materials and its sensitivity to organic solvents, these solvent etching involved conventional micro-ring preparation methods are difficult to apply to the perovskite material directly.<sup>[46–48]</sup> Recently, Cui group proposed a novel method of using polystyrene (PS) spheres as templates to guide the crystallization of inorganic perovskite CsPbBr<sub>3</sub> into micro-ring structures successfully.<sup>[45]</sup> Although CsPbBr<sub>3</sub> micro-ring arrays were obtained by this method, the subsequent removal of PS spheres with toluene was harmful to the morphology and the crystallinity of the micro-rings, which were crucial for the performance of the resonators.<sup>[49]</sup> Zhang et al. had achieved Ruddlesden–Popper perovskite micro-ring resonators with designable shape and size by a polydimethylsiloxane (PDMS) template with concave micro-ring structures. Because the micro-ring is formed by a closed waveguide with a width as small as a few micro-meters or even hundreds of nanometers, the template preparation requires complicated nano-patterning preparation technology, which increases the preparation cost and prolongs the manufacturing cycle of micro-ring resonator. In order to maximize the application of perovskite materials in integrated optics, it is urgent to find a simple method to realize perovskite-based micro-ring resonators.

Here, we propose a microstructure edge-guided crystallization method to fabricate organic–inorganic hybrid perovskite methylammonium lead bromide (MAPbBr<sub>3</sub>) micro-ring resonator arrays. The perovskite precursor solution is confined between the substrate and the PDMS template with micro-cylindrical structures, and the crystallization position and direction are controlled by the edge of the micro-cylindrical structures. By this method, large area and various shapes of ring resonators were obtained in a few minutes. Laser emission confirmed

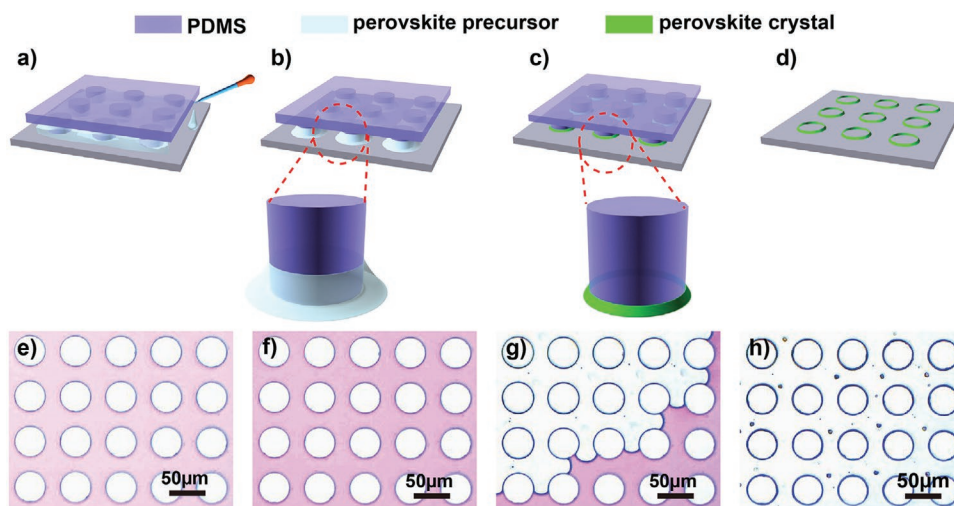


**Figure 1.** a–d) Schematic diagram of the preparation process of the MAPbBr<sub>3</sub> micro-ring arrays. e–h) In situ observation of micro-ring crystal growth process.

the high quality of these micro-ring resonators. By adjusting the size of the micro-ring, different modes of laser were realized. Our method broadens the range of material selection for the preparation of micro-rings.

The fabrication process of perovskite micro-rings based on edge-guided crystallization is shown in **Figure 1a–d**. First, PDMS film with micro-cylindrical arrays (as shown in **Figure S1**, Supporting Information) is tightly bonded to the substrate under suitable pressure. Release the pressure after making sure the micro-cylindrical arrays are in close contact with the substrate. During the shrinkage of the solution, the crystals tend to nucleate at the micro-scaled dirt on the substrate, resulting in unwanted small crystal grains. Therefore, in the preparation process, we must carefully clean the substrate to avoid providing extra nucleation point for perovskite. An appropriate amount of the perovskite precursor solution is then dropped on to the edge of the PDMS film and sandwiched between the substrate and the PDMS film, as shown in **Figure 1a**. At an appropriate heating temperature, the solution begins to evaporate, and the solution gradually shrinks, forming a circle of saturated solution at the edge of each micro-cylindrical, as shown **Figure 1b** and the enlarged diagram. As the solution continues to evaporate, the solution that is attached to the edge of the micro-cylindrical structure begins to crystallize. Because of the guidance of the cylindrical structure, crystallization proceeds along the periphery of the cylindrical structure. Therefore, a ring-shaped perovskite crystal is formed around the periphery of each micro-cylindrical structure, as shown in **Figure 1c** and the enlarged diagram. After the crystallization process is completed, the micro-structured PDMS film is peeled off and the perovskite ring array is obtained as shown in **Figure 1d**. In order to further understand the crystallization process of perovskite rings, we in situ observed this process under a microscope, as shown in **Movie S1**, Supporting Information, and **Figure 1e–h**. A red dye was added to the precursor solution for a clearer observation of the crystallization process. The crystallization process could be divided into four stages. First, the solution was distributed between the substrate and the PDMS film. As shown in **Figure 1e**, since the pro-

truding micro-cylindrical structures of the PDMS were tightly bonded to the substrate, the red solution was distributed outside the micro-cylinder structures. In the second stage, as the solvent gradually evaporated, the volume of the sandwiched solution was getting smaller and the solution concentration gradually increased, so the red color of the solution became deeper (**Figure 1f**). When the volume of the solution was small enough, the solution began to shrink, and during the shrinking process, a part of the high concentration solution adhered to the peripheries of the micro-cylinder structures, as shown in **Figure 1g**. In the final stage, as the solution continued to evaporate, the crystallization process proceeded rapidly around the micro-cylinders, and finally perovskite crystals with ring shape consistent with the micro-cylinder structures were formed (**Figure 1h**). Since the crystallization process proceeded around the micro-cylinders, although the width of the waveguide forming the micro-ring is small, the size of the micro-cylinders of the template does not need to be very small. Therefore, no sophisticated technique is required to prepare the template. This is beneficial to the low-cost and time-saving fabrication. Because the crystallization process is similar to the previously reported process and no steps that are detrimental to the properties of the crystal involved, the optical and electrical properties of the micro-ring crystal can match the results in literatures.<sup>[30]</sup>

Various characterization methods had been applied to characterize the MAPbBr<sub>3</sub> micro-ring arrays obtained by this method, as shown in **Figure 2**. As can be seen from the fluorescence microscope image (**Figure 2a**), the obtained micro-rings have bright green fluorescence under the excitation of 405 nm laser, and the luminescence of all micro-rings is uniform, suggesting that the obtained micro-rings possess high crystallization quality and uniform morphology. The black place represents the substrate without crystals, indicating that the crystallization position is precisely controlled by the PDMS template. From the scanning electron microscopic (SEM) image with low magnification in **Figure 2b**, it can be noticed that all the micro-rings have uniform morphology and size, which is attributed to the precise control of the PDMS template. From the high magnification SEM image (**Figure 2c**), it can be seen that the

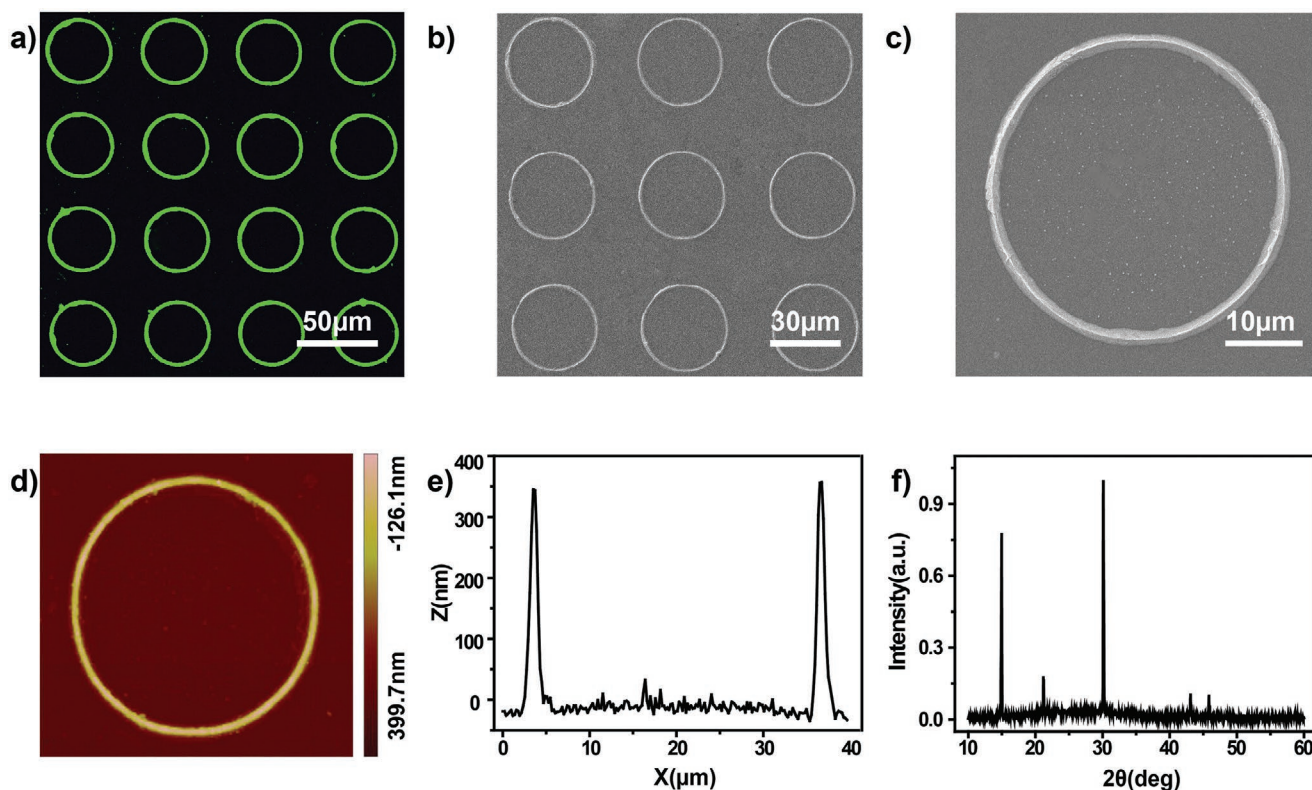


**Figure 2.** a) Fluorescence microscopy image of the highly aligned MAPbBr<sub>3</sub> micro-ring arrays. b) SEM image of highly aligned MAPbBr<sub>3</sub> micro-ring arrays. c) High magnification SEM image of a MAPbBr<sub>3</sub> micro-ring. d) AFM image of a single MAPbBr<sub>3</sub> micro-ring. e) Height profile of a single MAPbBr<sub>3</sub> micro-ring. f) XRD pattern of MAPbBr<sub>3</sub> micro-ring arrays.

micro-ring is a complete closed structure. Although the micro-ring is a crystal of a curved shape, there are no obvious cracks and open gaps in the micro-ring crystal, which can be observed from the enlarged SEM picture (Figure S2, Supporting Information). This complete ring structure and uniform surface morphology is beneficial to the confinement of light by the micro-ring, thereby ensuring the function of the micro-ring as a resonator. The morphology of the micro-ring was further characterized by atomic force microscopy (AFM), as shown in Figure 2d. The micro-ring not only has a perfect circular shape but also a uniform height, which is presented in the lateral height profile in Figure 2e. These characterizations demonstrate the complete ring structure of the micro-rings obtained by this method and suggest their crystallinity, which is confirmed by X-ray diffraction (XRD), as shown in Figure 2f. As a controlled experiment, the XRD pattern of the perovskite thin film prepared by drop coating method is shown in the Figure S3, Supporting Information. We found that this microstructure edge-guided crystallization method has no negative effect on the crystallinity of perovskite micro-ring. The uniform distribution of Pb, Br, and Si elements in perovskite micro-rings is displayed in EDS mapping in Figure S4, Supporting Information. The uniform distribution of Pb and Br elements in micro-ring at an atomic ratio of  $3.57:11.6 \approx 1:3$  is consistent with the atom ratio in MAPbBr<sub>3</sub>. The black ring shape in Figure S4d, Supporting Information, proves that there are no cracks and open gaps in the micro-ring. The absorption and PL spectra of the micro-ring arrays were shown in Figure S5, Supporting Information.

The concentration of the precursor solution is a very critical factor for the preparation of the micro-rings. We have found that when the concentration of the precursor is too low, the amount of the solute is too small to form a complete ring structure. As shown in Figure S6a, Supporting Information, when the concentration is below 15 wt%, the obtained micro-rings are incomplete. When the concentration is too high, a large amount of solute will result in a large amount of bulk crystals and unwanted grains. As shown in Figure S6b, Supporting Information, when the concentration is higher than 30%, a bulk crystal is distributed around the PDMS micro-cylinder structures to form a crystal thin film with cylindrical concave structures. Therefore, we used a precursor solution with a concentration of about 25% to prepare the micro-ring arrays. Although a high temperature can shorten the crystallization time, a higher temperature will cause the template to separate from the substrate driven by the large amount of solvent vapor, making the crystallization direction and position no longer controlled by the template. Moreover, fast crystallization process caused by the high temperature will lead to disorder and random nucleation position (Figure S7, Supporting Information). Hence we choose 60 °C to prepare the micro-ring resonators.

In practical applications, in addition to the ring-shaped resonator, other shapes of resonators are also very important. Therefore, the preparation of other shapes of micro-rings is also urgently required. However, by using PS spheres as templates, ring structures of other shapes cannot be obtained except for the circular micro-ring structure. Here, by simply changing the

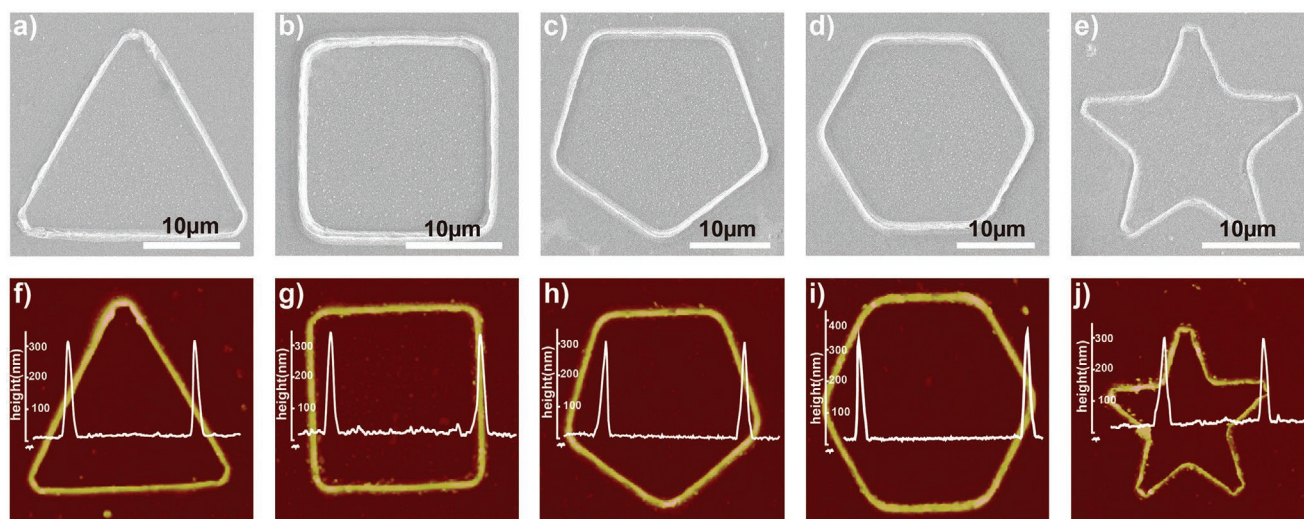


**Figure 3.** a–e) SEM images of MAPbBr<sub>3</sub> micro-rings with different shapes of triangle, square, pentagon, hexagon, and pentagram, respectively. f–j) AFM images of MAPbBr<sub>3</sub> micro-rings with different shapes of triangle, square, pentagon, hexagon, and pentagram, respectively.

shapes of the micro-columnar structures of the PDMS templates, we can get the micro-ring perovskite crystals with different shapes. As shown in **Figure 3**, the perovskite micro-rings with the shapes of triangle, square, pentagon, hexagon, and pentagram were obtained by using PDMS templates with micro-columnar structures of triangle, square, pentagon, hexagon, and pentagram respectively. Our method provides an opportunity for the application of perovskite materials in integrated optics.

In order to prove the excellent optical properties of the perovskite micro-ring obtained, the micro-cavity effect was studied, as shown in **Figure 4**. **Figure 4a** shows a diagram of a perovskite micro-ring pumped by a femtosecond laser. The excitation laser with a wavelength of 400 nm and a frequency of 1 kHz is focused by an objective lens ( $40 \times 0.65$ ) to pump the micro-ring on the glass substrate. **Figure 4b** shows the fluorescence spectrum of the micro-ring under different intensities of the pumping laser. At low pumping intensity, the micro-ring exhibits a wide spontaneous emission. When the pump intensity exceeded a threshold, a series of sharp peaks were observed, which proved the cavity effect of the micro-ring. Because of the confinement of the light by the micro-ring resonator, only the light of specific wavelength could be amplified and output, so the spectrum was comb-shaped with multiple narrow peaks. The relationship between peak intensity of the fluorescence and the pumping intensity was depicted in **Figure 4c**. An obvious threshold of  $70.8 \mu\text{J cm}^{-2}$  was observed, which proved the laser emission behavior of the micro-ring. In addition to the fluorescence intensity, the evaluation of the full width at half-maximum (FWHM) is also an important data to show the threshold of the laser emission of the micro-ring arrays. As shown in **Figure 4c**, when the intensity of the pump light reached the threshold, the FWHM of the emission spectrum decreased sharply to 1 nm or even smaller. The FWHM is lower than the typical value of amplified spontaneous emission in organic materials, which is about 10 nm. Quality factor, an important parameter to judge the quality of a micro-resonator, according to the formula  $Q = \lambda/\Delta\lambda$  ( $\lambda$  is the peak wavelength

and  $\Delta\lambda$  is the value of FWHM), was calculated to be around 885. Compared with other perovskite-based micro-cavity, the  $Q$  value of this micro-ring is not particularly high, but it is enough to prove that the micro-ring structure can realize the function of a resonator. In future, we will focus on improving the quality of micro-ring, so as to realize its application in the field of integrated optoelectronics. In addition, by changing the size of the micro-cylindrical structure of the PDMS template, micro-rings of different sizes were obtained (**Figure S8**, Supporting Information), so that mode spaces ( $\Delta\lambda_m$ ) of the micro-ring laser could be regulated. According to the formula  $\Delta\lambda_m = \lambda^2/L[n - \lambda(dn/d\lambda)]$ , in which  $n$  is the refractive index and  $L$  is the circumference of the micro-ring,  $\Delta\lambda_m$  is inversely proportional to the diameter of the micro-ring. As shown in **Figure 4d**, micro-ring laser resonators with  $\Delta\lambda_m$  of 1.7, 2.3, and 4.4 nm and even single mode were realized in micro-rings of different diameters. The relationship of  $\Delta\lambda_m$  and the diameter of the micro-ring was shown in **Figure S9**, Supporting Information. The linear relationship also proved the micro-cavity effect of the micro-ring. The above results confirm that the perovskite micro-rings obtained by this method can be used as excellent resonators.

In summary, a simple method for fabrication of shape-designable and size-tunable perovskite micro-rings has been demonstrated. By this method, large area perovskite micro-ring arrays with uniform morphology were fabricated. By simply changing the shape and size of PDMS template microstructures, the shape and size of micro-rings can be accurately adjusted. Furthermore, the optical resonator functions of these micro-rings have been verified by micro-ring laser emission. Our method provides an opportunity for the application of perovskite materials in integrated optics.

## Supporting Information

Supporting Information is available from the Wiley Online Library or from the author.

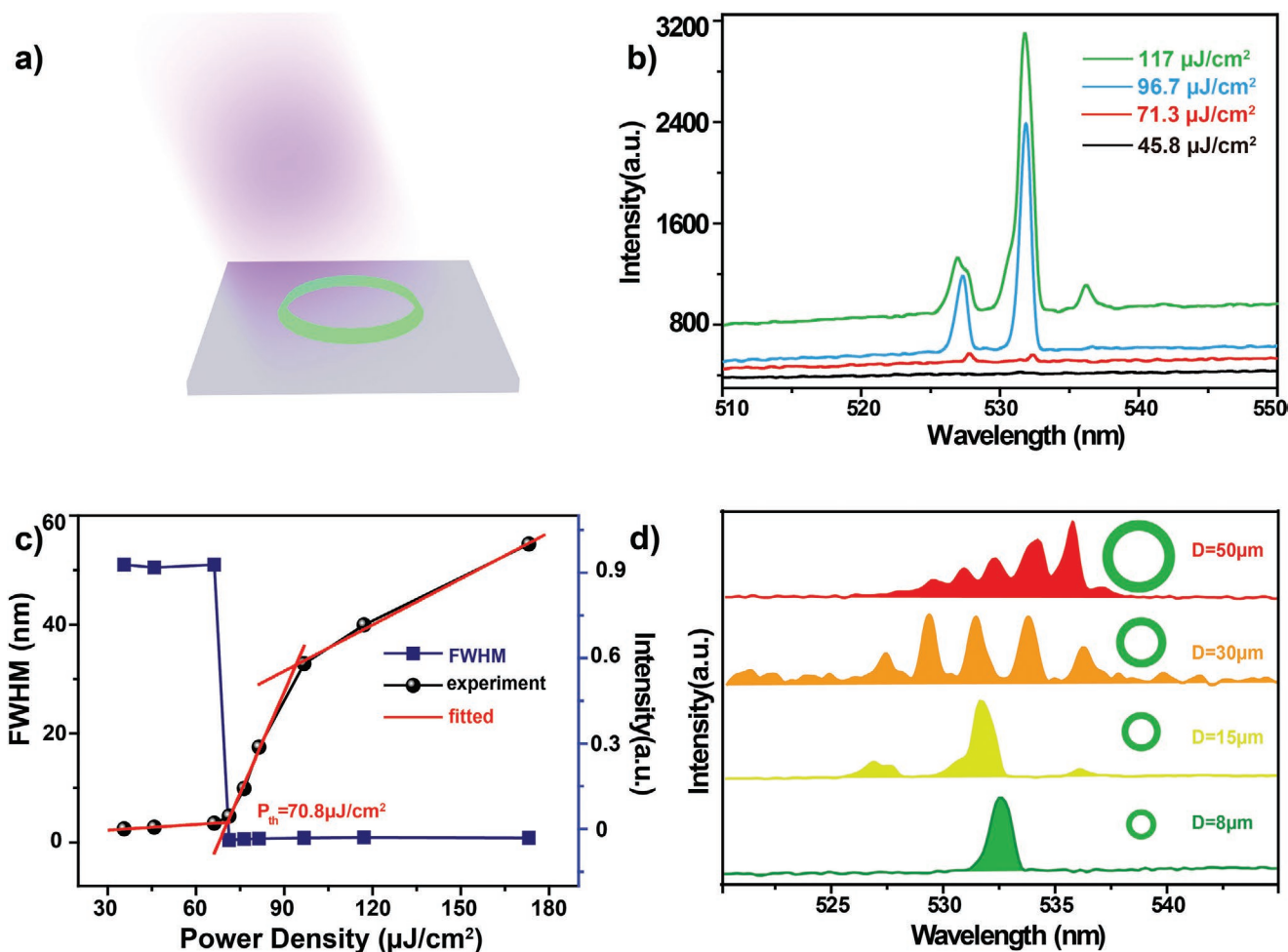


**Figure 4.** a) A diagram of the MAPbBr<sub>3</sub> micro-ring pumped by a 400 nm femtosecond laser. b) Fluorescence spectra of the MAPbBr<sub>3</sub> micro-ring under pumped at different light intensity. c) The relationship between peak intensity of the fluorescence of the MAPbBr<sub>3</sub> micro-ring and the pumping intensity. d) Laser emission spectra of different modes in micro-rings of different diameters.

## Acknowledgements

This work was supported by the National Key Research and Development Program of China and the National Natural Science Foundation of China (NSFC) under Grants #61435005, #61590930, #21903035, #61825502, and #61827826.

## Conflict of Interest

The authors declare no conflict of interest.

## Keywords

edge-guided crystallization method, microlaser arrays, micro-ring resonators, organic–inorganic hybrid perovskites

Received: January 21, 2020

Revised: March 3, 2020

Published online:

- [1] B. T. Ren, G. C. O. Yuen, S. B. Deng, L. Jiang, D. J. Zhou, L. L. Gu, P. Xu, M. Zhang, Z. Y. Fan, F. S. Y. Yueng, R. S. Chen, H. S. Kwok, G. J. Li, *Adv. Funct. Mater.* **2019**, 29, 9.
- [2] Y. Q. Bie, G. Grosso, M. Heuck, M. M. Furchi, Y. Cao, J. B. Zheng, D. Bunandar, E. Navarro-Moratalla, L. Zhou, D. K. Efetov, T. Taniguchi, K. Watanabe, J. Kong, D. Englund, P. Jarillo-Herrero, *Nat. Nanotechnol.* **2017**, 12, 1124.
- [3] K. Liao, X. Y. Hu, Y. K. Cheng, Z. C. Yu, Y. X. Xue, Y. Chen, Q. H. Gong, *Adv. Opt. Mater.* **2019**, 7, 30.
- [4] Y. Hu, X. Luo, Y. Chen, Q. Liu, X. Li, Y. Wang, N. Liu, H. Duan, *Light: Sci. Appl.* **2019**, 8, 86.
- [5] J. N. Wang, Y. Q. Liu, Y. L. Zhang, J. Feng, H. Wang, Y. H. Yu, H. B. Sun, *Adv. Funct. Mater.* **2018**, 28, 8.
- [6] X. Guo, Y. Ding, Y. Duan, X. Ni, *Light: Sci. Appl.* **2019**, 8, 123.
- [7] W. L. Liu, M. Li, R. S. Guzzon, E. J. Norberg, J. S. Parker, M. Z. Lu, L. A. Coldren, J. P. Yao, *Nat. Commun.* **2017**, 8, 6.
- [8] M. Xin, N. Li, N. Singh, A. Ruocco, Z. Su, E. S. Magden, J. Notaros, D. Vermeulen, E. P. Ippen, M. R. Watts, F. X. Kärtner, *Light: Sci. Appl.* **2019**, 8, 122.
- [9] Y. Sun, W. Shin, D. A. Laleyan, P. Wang, A. Pandey, X. H. Liu, Y. P. Wu, M. Soltani, Z. T. Mi, *Opt. Lett.* **2019**, 44, 5679.

- [10] K. G. Cognée, H. M. Doleman, P. Lalanne, A. F. Koenderink, *Light: Sci. Appl.* **2019**, *8*, 115.
- [11] Y. Zheng, M. H. Pu, A. L. Yi, X. Ou, H. Y. Ou, *Opt. Lett.* **2019**, *44*, 5784.
- [12] H. Gu, H. Gong, C. Wang, X. Sun, X. Wang, Y. Yi, C. Chen, F. Wang, D. Zhang, *Sensors* **2019**, *19*, 5038.
- [13] H. Zhou, Y. Geng, W. Cui, S.-W. Huang, Q. Zhou, K. Qiu, C. Wei Wong, *Light: Sci. Appl.* **2019**, *8*, 50.
- [14] H. H. Zhang, Q. Liao, Y. S. Wu, Z. Y. Zhang, Q. G. Gao, P. Liu, M. L. Li, J. N. Yao, H. B. Fu, *Adv. Mater.* **2018**, *30*, 8.
- [15] Z. Cao, B. Yao, C. Qin, R. Yang, Y. Guo, Y. Zhang, Y. Wu, L. Bi, Y. Chen, Z. Xie, G. Peng, S.-W. Huang, C. W. Wong, Y. Rao, *Light: Sci. Appl.* **2019**, *8*, 107.
- [16] S. C. Yang, Y. Wang, H. D. Sun, *Adv. Opt. Mater.* **2015**, *3*, 1136.
- [17] S. Matsuura, N. Yamasaku, Y. Nishijima, S. Okazaki, T. Arakawa, *Sensors* **2020**, *20*, 96.
- [18] E. Stankevicius, E. Daugnoraitė, I. Ignatjev, Z. Kuodis, G. Niaura, G. Raciukaitis, *Appl. Surf. Sci.* **2019**, *497*, 143752.
- [19] X. Tu, S. L. Chen, C. L. Song, T. Y. Huang, L. J. Guo, *IEEE Photonics J.* **2019**, *11*, 10.
- [20] T. Ling, L. Y. Liu, Q. H. Song, L. Xu, W. C. Wang, *Opt. Lett.* **2003**, *28*, 1784.
- [21] B. J. Huang, C. L. Wu, Y. H. Lin, H. Y. Wang, C. T. Tsai, C. H. Cheng, Y. C. Chi, P. H. Chang, C. I. Wu, R. A. Soref, G. R. Lin, *Adv. Mater. Technol.* **2017**, *2*, 15.
- [22] C. Zhang, C. L. Zou, Y. Zhao, C. H. Dong, C. Wei, H. L. Wang, Y. Q. Liu, G. C. Guo, J. N. Yao, Y. S. Zhao, *Sci. Adv.* **2015**, *1*, 7.
- [23] K. Bando, H. Fujii, K. Mizuno, K. Narushima, A. Miyazaki, F. Sasaki, S. Hotta, H. Yanagi, *ChemNanoMat* **2018**, *4*, 936.
- [24] C. H. Kang, I. Dursun, G. Liu, L. Sinatra, X. Sun, M. Kong, J. Pan, P. Maity, E.-N. Ooi, T. K. Ng, O. F. Mohammed, O. M. Bakr, B. S. Ooi, *Light: Sci. Appl.* **2019**, *8*, 94.
- [25] D. Yin, N. R. Jiang, Y. F. Liu, X. L. Zhang, A. W. Li, J. Feng, H. B. Sun, *Light: Sci. Appl.* **2018**, *7*, 8.
- [26] W. Hu, H. Cong, W. Huang, Y. Huang, L. Chen, A. Pan, C. Xue, *Light: Sci. Appl.* **2019**, *8*, 106.
- [27] S. Li, Y. Li, Z. F. Shi, L. Z. Lei, H. F. Ji, D. Wu, T. T. Xu, X. J. Li, G. T. Du, *Sol. Energy Mater. Sol. Cells* **2019**, *191*, 275.
- [28] S.-X. Li, G.-P. Zhang, H. Xia, Y.-S. Xu, C. Lv, H.-B. Sun, *Nanoscale* **2019**, *11*, 18272.
- [29] R. Su, J. Wang, J. X. Zhao, J. Xing, W. J. Zhao, C. Diederichs, T. C. H. Liew, Q. H. Xiong, *Sci. Adv.* **2018**, *4*, 6.
- [30] Q. Zhang, S. T. Ha, X. F. Liu, T. C. Sum, Q. H. Xiong, *Nano Lett.* **2014**, *14*, 5995.
- [31] X. J. Li, X. J. Zhang, H. F. Li, T. H. Liu, D. D. Zhao, C. Hang, G. C. Xing, Z. K. Tang, *Adv. Opt. Mater.* **2019**, *7*, 9.
- [32] X. X. He, P. Liu, H. H. Zhang, Q. Liao, J. N. Yao, H. B. Fu, *Adv. Mater.* **2017**, *29*, 8.
- [33] J. G. Feng, X. X. Yan, Y. F. Zhang, X. D. Wang, Y. C. Wu, B. Su, H. B. Fu, L. Jiang, *Adv. Mater.* **2016**, *28*, 3732.
- [34] Q. Zhang, R. Su, X. F. Liu, J. Xing, T. C. Sum, Q. H. Xiong, *Adv. Funct. Mater.* **2016**, *26*, 6238.
- [35] J. Xing, X. F. Liu, Q. Zhang, S. T. Ha, Y. W. Yuan, C. Shen, T. C. Sum, Q. H. Xiong, *Nano Lett.* **2015**, *15*, 4571.
- [36] Z. Y. Gu, K. Y. Wang, W. Z. Sun, J. K. Li, S. Liu, Q. H. Song, S. M. Xiao, *Adv. Opt. Mater.* **2016**, *4*, 472.
- [37] B. Tang, H. X. Dong, L. X. Sun, W. H. Zheng, Q. Wang, F. F. Sun, X. W. Jiang, A. L. Pan, L. Zhang, *ACS Nano* **2017**, *11*, 10681.
- [38] B. R. Sutherland, S. Hoogland, M. M. Adachi, C. T. O. Wong, E. H. Sargent, *ACS Nano* **2014**, *8*, 10947.
- [39] Q. Wei, X. J. Li, C. Liang, Z. P. Zhang, J. Guo, G. Hong, G. C. Xing, W. Huang, *Adv. Opt. Mater.* **2019**, *7*, 33.
- [40] J. G. Feng, X. X. Yan, Y. Liu, H. F. Gao, Y. C. Wu, B. Su, L. Jiang, *Adv. Mater.* **2017**, *29*, 9.
- [41] G. Wachter, S. Kuhn, S. Minniberger, C. Salter, P. Asenbaum, J. Millen, M. Schneider, J. Schalko, U. Schmid, A. Felgner, D. Hüser, M. Arndt, M. Trupke, *Light: Sci. Appl.* **2019**, *8*, 37.
- [42] C. Han, M. Lee, S. Callard, C. Seassal, H. Jeon, *Light: Sci. Appl.* **2019**, *8*, 40.
- [43] W. Bogaerts, P. De Heyn, T. Van Vaerenbergh, K. De Vos, S. K. Selvaraja, T. Claes, P. Dumon, P. Bienstman, D. Van Thourhout, R. Baets, *Laser Photonics Rev.* **2012**, *6*, 47.
- [44] W. Wang, Y. Q. Liu, Y. Liu, B. Han, H. Wang, D. D. Han, J. N. Wang, Y. L. Zhang, H. B. Sun, *Adv. Funct. Mater.* **2017**, *27*, 8.
- [45] J. K. Xu, S. H. Xu, Z. Q. Qi, C. L. Wang, C. G. Lu, Y. P. Cui, *Nanoscale* **2018**, *10*, 10383.
- [46] X. Y. Yang, J. Wu, T. H. Liu, R. Zhu, *Small Methods* **2018**, *2*, 10.
- [47] X. Z. Xu, X. J. Zhang, W. Deng, J. S. Jie, X. H. Zhang, *Small Methods* **2018**, *2*, 19.
- [48] J. A. Christians, P. A. M. Herrera, P. V. Kamat, *J. Am. Chem. Soc.* **2015**, *137*, 1530.
- [49] C. C. Boyd, R. Cheacharoen, T. Leijtens, M. D. McGehee, *Chem. Rev.* **2019**, *119*, 3418.